Filtered density-function modeling for large-eddy simulations of turbulent reacting flows

By Chong M. Cha AND Philippe Trouillet

1. Motivation and objectives

Large-eddy simulations (LES) have become practical for describing turbulent mixing in flows of engineering interest. At high Reynolds numbers, the response of small-scale mixing dynamics to the large-scale eddies is thought to be universal. Since only the unresolved small-scale (or subgrid-scale) processes require modeling in an LES, it is believed to be more robust than Reynolds-averaged (RANS) turbulence modeling, which also models the large-scale dynamics and hence must be tuned for different geometries.

In turbulent reacting flows of practical interest, the chemical scales can be even smaller than the smallest turbulence scales. With initially-nonpremixed reactants, the separation of chemical and turbulence scales allows a presumed beta PDF and the steady flamelet model to describe the subgrid-scale mixing and reaction processes, respectively, in a LES (Cook & Riley 1994; Cook *et al.* 1997; Cook & Riley 1997). (The unsteady response of flamelets to residence-time effects in an LES has been accounted for by Pitsch & Steiner (2000*a*,*b*).) The feedback of these subgrid-scale processes create significant density changes which impact the large-scale dynamics which, in turn, drive the modeled small-scale processes. Thus, a breakdown of flamelet modeling at the subgrid scale, for example when local extinction and reignition events become significant (Sripakagorn *et al.* 2000), would invalidate the entire LES calculation.

With regard to local extinction, fluctuations due to internal intermittency have yet to be accounted for in an LES of any turbulent reacting flow. Although of little importance for first- and second-order moment predictions without reaction (Pope 2000), their effect has a nontrivial impact on stable burning, either in a flamelet or distributed reaction mode. This is especially important with present implementations based on flamelet modeling, where no entirely satisfactory mechanism for reignition yet exists (Pitsch *et al.* 2002).

The present work focuses on the filtered-density-function (FDF) approach and its variants (Colucci *et al.* 1999; Jaberi *et al.* 1999). In the FDF approach, subgrid-scale processes are described by Lagrangian Monte Carlo calculations of the "large-eddy probability density function" (Gao & O'Brien 1993) for, most generally, the joint large-eddy PDF of velocity, the reacting scalars, and the dissipation. (The additional dissipation dimension would be required to account for intermittency effects (Pope 1990).)

The dominant mechanism by which local reignition occurs in a turbulent flow is not completely understood. DNS with initially-nonpremixed reactants in three-dimensional turbulence (Sripakagorn *et al.* 2000) seem to suggest that reignition occurs primarily by convective transport. Alternatively, triple-flame propagation may be the dominant mechanism, as seen in two-dimensional "turbulence" simulations of autoignition (Domingo & Vervisch 1996). Accounting for the latter mechanism in an FDF approach may be prohibitively expensive computationally. For turbulence at high Reynolds number, the

expectation is that the former mechanism will dominate (Hewson & Kerstein 2001). Reignition by distributed combustion can be described by the FDF approach.

These potentially attractive features of the family of FDF approaches, e.g., for describing local extinction and reignition, motivate the present work. "FDF" is henceforth used to represent any of the variations of the transported large-eddy PDF approaches (Colucci *et al.* 1999; Jaberi *et al.* 1999) that also exist analogously in the RANS case (Pope 1985). In the FDF approach, the time-dependent structure of the turbulence down to the Taylor scale is reproduced; changes at finer resolution are accounted for by modeling the effective diffusion at the unresolved scales. This is represented by the conditionally-averaged molecular mixing term in the joint PDF equation. Closure is obtained by modeling this term with the available single-point information, which then requires the spatial correlation to be prescribed *via* a characteristic length or time scale. Current micro-mixing models for reacting scalars ignore the influence of chemistry on this time scale by using the turbulent time scale of a conserved scalar in place of the reacting-scalar time scale. This implicitly assumes distributed combustion. With realistic, Arrhenius kinetics, the large activation temperature steepens the local gradients of a reacting scalar, decreasing its length or time scale as compared to the conserved scalar under the same turbulent velocity field. Thus, for sufficiently fast chemistry, the generally used estimate of substituting the time scale of the reacting scalar by that of a conserved scalar can significantly overestimate the true mixing time for the reacting scalar.

An improved approach for modeling the time scale of a turbulent reacting scalar, valid in both the flamelet and distributed-combustion limits, has been developed by Cha (2001) and Cha & Trouillet (2002) within a RANS framework. The model can readily be applied to any existing micro-mixing model where the time scales of the reacting scalars appear explicitly. This would include classic linear-mean-square estimation (LMSE) (Dopazo 1975), extended LMSE (Sabel'nikov & Gorokhovski 2001), and the variants of Curl's approach (Norris & Pope 1991), to name a few. The issues arising from its application with a RANS turbulence model are discussed in Cha (2001) and Cha & Trouillet (2002). For inhomogeneous turbulent flows, the assumption of local homogeneity and isotropy within a computational volume was made.

The objective of the present work is to validate the analogous time-scale model for a reacting scalar in an LES framework. At present, the phenomena of local extinction and reignition are not addressed. Note that to describe local extinction with a mixing-limited combustion mode, a subgrid-scale mixing model must first be able to treat flamelet combustion, by definition. The new modeling presented in this paper addresses this specific issue. The expectation is better performance in a LES framework as compared to the RANS case, as the assumption of local homogeneity and isotropy below the Taylor scale (for LES) *vis-á-vis* at the sub-integral scale (for RANS) would be more accurate. The modeling validation is performed using the direct numerical simulation (DNS) of a turbulent reacting jet (Boersma 1999), which was also used for the RANS validation case in Cha & Trouillet (2002).

The paper is organized as follows. In the next section, the numerical experiment of Boersma (1999), which simulates a reacting jet with a single-step reaction, is described. In section 3, the micro-mixing model is described within the LES framework. In section 4, results of the modeling study using the DNS of the jet flame are presented and discussed. Conclusions are given in section 5.

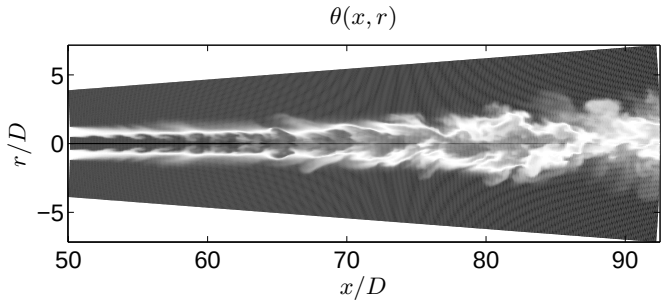

FIGURE 1. Temperature field from the turbulent reacting jet DNS of Boersma (1999). The planar slice shown lies on the jet centerline. Axial and radial distances are nondimensionalized by D, the jet nozzle diameter. The Reynolds number based on fuel-nozzle exit conditions is 4,000.

2. Numerical experiment

The *a priori* validation study uses the DNS of a turbulent reacting jet performed by Boersma (1999). Briefly, the Reynolds number based on fuel-nozzle exit conditions is 4,000. A global, second-order, irreversible reaction where one mole of fuel (F) reacts with one mole of oxidizer (O) to form two moles of product (P) is considered:

$$\mathrm{F} + \mathrm{O} \rightarrow 2\mathrm{P}. \tag{2.1a}$$

The chemical source terms for fuel, oxidizer, and product are $\dot{s}_\mathrm{F} = -\dot{s}$, $\dot{s}_\mathrm{O} = -\dot{s}$, and $\dot{s}_\mathrm{P} = 2\dot{s}$, respectively, where

$$\dot{s} = k\rho\psi_\mathrm{F}\psi_\mathrm{O} \tag{2.1b}$$

$$k = A\exp\left[-\frac{\mathrm{Ze}(1-\theta)}{1-\alpha(1-\theta)}\right]. \tag{2.1c}$$

Here, ψ_j represents the mass fraction of the j-th species ($j = $ F, O, or P), ρ is the mixture density, A is an effective frequency factor, $\alpha \equiv (T_f - T_\infty)/T_f$ is the heat-release parameter, $\mathrm{Ze} \equiv \alpha T_a/T_f$ is the Zeldovich number, and $\theta \equiv (T - T_\infty)/(T_f - T_\infty)$ is the normalized temperature with T_a, T_f, and T_∞ the activation, flame, and reference temperatures, respectively. The chemical-kinetic rate parameters were chosen to approximate methane/air combustion with 300 K temperatures for the initially segregated F and O streams: $A = 10^5$, $\alpha = 0.8$, and $\mathrm{Ze} = 8.0$. The Schmidt number is 0.75 and Lewis numbers are unity. Heat release is accounted for, with a maximum density ratio of approximately 5. The molecular diffusivities and viscosity are temperature-dependent. See Boersma (1999) for details of the simulation.

Bilger's mixture fraction for this system can be written as

$$\xi = \frac{1}{2}(\psi_\mathrm{F} - \psi_\mathrm{O} + 1),$$

one of three linear combinations of the reactive scalars (Shvab-Zeldovich coupling functions) for this case, which eliminates the chemical source term and conveniently normalizes this passive scalar such that it is unity in pure fuel and zero in pure oxidizer (Bilger 1980). For the present case, fuel and oxidizer are in stoichiometric proportion at $\xi = \xi_\mathrm{st} = 1/2$. The dissipation rate of passive-scalar energy is represented by $\chi \equiv 2\mathcal{D}(\nabla\xi)^2$, where $\mathcal{D}$ is the diffusion coefficient of ξ. In a turbulent flow, χ reduces the variance of ξ, thus characterizing the rate of mixing which drives ξ to its mean value. For nonpremixed systems, the local $\chi(t, \xi)$ describes the flux of fuel and oxidizer into the reaction zone at $\xi = \xi_\mathrm{st}$ (Peters 1984). For the present kinetic rate parameters, if χ exceeds a value of 4.2 sec^{-1}, the rate of mixing in ξ phase space exceeds the chemical

production rate and extinguishes the flame. That is, 4.2 is the quenching value of the scalar dissipation rate, $\chi = \chi_q$, as given by the steady flamelet solution (Peters 1984).

Figure 1 shows the typical, instantaneous spatial distribution of the temperature field, θ, from the DNS of the jet flame. The typical LES computational grid would not resolve the entire range of turbulent scales shown. Accounting for the unresolved turbulent structure is a turbulence modeling issue. Accounting for the unresolved spatial structure of the reactive scalars is a combustion modeling issue and is discussed next.

3. Modeling

Within an LES computational volume, the transport equation for the subgrid-scale variance of the j-th reacting scalar can be written as

$$\frac{1}{\langle\psi_j'^2\rangle}\frac{d\langle\psi_j'^2\rangle}{dt} - \frac{\langle\dot{s}_j'\psi_j'\rangle}{\langle\psi_j'^2\rangle} = -\frac{\langle 2\mathcal{D}(\nabla\psi_j)^2\rangle}{\langle\psi_j'^2\rangle} \equiv \frac{1}{T_j}. \tag{3.1}$$

where local homogeneity and isotropy have been assumed. Here, $\langle(\cdot)\rangle$ denotes the LES filtering operation, $\langle\psi_j'^2\rangle \equiv \langle\psi_j^2\rangle - \langle\psi_j\rangle^2$ is the subgrid-scale variance, $\langle\dot{s}_j'\psi_j'\rangle \equiv \langle\dot{s}_j\psi_j\rangle - \langle\dot{s}_j\rangle\langle\psi_j\rangle$ is the subgrid-scale covariance of $\dot{s}_j$, the chemical source term of the j-th species, with ψ_j, and $\langle 2\mathcal{D}(\nabla\psi_j)^2\rangle \equiv \chi_j$ is the scalar dissipation rate of the j-th scalar. The time scale of the j-th reactive scalar, T_j, is then $T_j = \langle\psi_j'^2\rangle/\langle\chi_j\rangle$. If $\dot{s}_j = 0$, then ψ_j is a conserved or passive scalar, ξ, by definition. We denote the time scale of the passive scalar by $T = \langle\xi'^2\rangle/\langle\chi\rangle$, which can be related to the time scale of the turbulence (Pope 1985).

The limit of infinitely-fast chemistry of a simple chemistry case is worth elucidating: For a global, one-step, irreversible reaction, $\dot{s}_j = 0$ outside an infinitely-thin reaction zone, transport is then governed by turbulent mixing and $T_j = T$. In the frozen chemistry limit, $\dot{s}_j \equiv 0$ and trivially $T_j = T$. Current particle-interaction models used in Lagrangian Monte Carlo simulations are valid in these limits.

In the slow-chemistry limit, the transport of a reacting scalar is governed primarily by advective stirring (distributed combustion) and $T_j \approx T$. Then, for unity Schmidt number, the time scale of ψ_j can be constructed with the relevant turbulent length scale and diffusivity. For an LES, $T \sim \Delta^2/\nu_t$ (Jaberi *et al.* 1999), where Δ is the grid width and ν_t the subgrid eddy viscosity. In the fast, but not infinitely fast, chemistry limit (flamelet combustion), T_j can deviate from T by an order of magnitude over an integral time scale (Cha 2001; Cha & Trouillet 2002);

Thus, current particle-interaction models, which replace the mixing time scale of a reactive scalar by the turbulence time scale, are not valid in this limit. Formulation of the model for the T_j/T ratio for the LES case readily follows from the work of Cha (2001) and Cha & Trouillet (2002). The model is based on (i) mapping closure, which describes the effects from the mixing at the sub-Taylor scale in this LES case, and (ii) flamelet modeling, which relates the mapping functions for the passive and reactive scalars. The synthesis of these modeling elements is described in the following subsections.

3.1. *Passive-scalar mixing*

Mapping closure was originally conceived by Chen *et al.* (1989) to describe the probability distribution of a passive scalar field advected by Navier-Stokes turbulence. Briefly, mapping closure provides the transformation from a standard, Gaussian reference field, z_0, enforcing the exact transport equation for ξ of a binary mixing problem. Denoting the

transformation by $z_0 \xrightarrow{X} \xi$, the generally nonlinear mapping, X, then describes the deviation of p_ξ from the standard, Gaussian distribution of z_0, $p_{z_0} \equiv (1/2\pi)^{1/2}\exp(-z_0^2/2)$. Using X, the fine-scale mixing and probability distribution of ξ at scales below which $\langle(\cdot)\rangle$ is defined can be directly calculated using (Chen *et al.* 1989)

$$\langle \mathcal{D}(\nabla\xi)^2|\xi=\eta\rangle = \langle \mathcal{D}(\nabla\xi)^2\rangle \frac{(\partial X/\partial z_0)^2}{\langle(\partial X/\partial z_0)^2\rangle} \tag{3.2a}$$

$$p_\xi = \frac{1}{\partial X/\partial z_0} p_{z_0}, \tag{3.2b}$$

respectively. With local homogeneity and isotropy assumed within an LES computational cell, the analytical developments of Gao (1991*b*,*a*) and O'Brien & Jiang (1991) can be applied to give (Cha & Trouillet 2002)

$$X(z_0) = \xi^- + \frac{1}{2}\left(\xi^+ - \xi^-\right)\left\{1 + \mathrm{erf}\left[\frac{z_0}{\sqrt{2}\Sigma} - \beta \mathrm{erf}^{-1}\left(2\frac{\xi^+ - \langle\xi\rangle}{\xi^+ - \xi^-} - 1\right)\right]\right\} \tag{3.3a}$$

$$p_\xi(\eta) = \Sigma \exp\left\{\gamma^2 - \Sigma\left[\gamma + \beta \mathrm{erf}^{-1}\left(2\frac{\xi^+ - \langle\xi\rangle}{\xi^+ - \xi^-} - 1\right)\right]^2 - \log\left(\xi^+ - \xi^-\right)\right\} \tag{3.3b}$$

valid for each LES computational cell, with the spatial average $\langle\xi\rangle$, subgrid rms ξ' and $\langle\chi\rangle$ given by a suitable SGS turbulence model. Here, ξ^- and ξ^+ are the minimum and maximum values of ξ in each LES computational cell, Σ is determined from the subgrid-scale variance, η is the sample space variable of ξ, $\gamma \equiv \mathrm{erf}^{-1}(2(\eta-\xi^-)/(\xi^+-\xi^-)-1)$, and $\beta \equiv (1+1/\Sigma^2)^{1/2}$. In an LES using the FDF approach, the values of $\langle\xi\rangle$ and $\langle\xi'^2\rangle$ are known at each time in each cell. Estimates of ξ^- and ξ^+ are known from the information carried by the ensemble of notional particles.

The current standard modeling practice in LES calculations is to construct passive-scalar mixing statistics from $\langle\xi\rangle$ and $\xi' \equiv \langle\xi'^2\rangle^{1/2}$ only, using an assumed beta PDF shape to approximate the large-eddy PDF. *A priori* studies show that the assumed beta PDF distribution well approximates filtered DNS data of homogeneous turbulence (Cook & Riley 1994) and the present, nonhomogeneous case of the turbulent reacting jet (Wall *et al.* 2000). For practical purposes, (3.3*b*) with $\xi^- = 0$ and $\xi^+ = 1$ yields distributions essentially identical to the beta PDF (Cha & Trouillet 2002). (This can be readily verified by direct calculation, substituting the various possible values of $\langle\xi\rangle \in [0,1]$ and $\xi'^2 \in [0, 1/4]$ into (3.3*b*), the PDF from mapping closure, against the well-known presumed beta PDF.)

The beta PDF has not been related to first principles: its motivation lies only in describing a bounded random variable whose first and second moments can be enforced by an LES (or RANS) turbulence model. In contrast, mapping closure describes the assumptions leading to (3.3*b*), beginning with the exact transport equation for ξ (Chen *et al.* 1989). In the late stages of mixing ($\xi' \to 0$), the two approaches are demonstrably consistent. For $\xi' \to 0$, or equivalently, $\langle\chi\rangle \to 0$, the beta PDF can be shown to asymptote to the Gaussian distribution (Girimaji 1991). This behavior is the fundamental modeling assumption on which mapping closure is based. In the late stages of mixing, the mapping becomes linear and (3.3*b*) asymptotes to a normal distribution, $\Sigma p_\xi((\eta - \langle\xi\rangle)/\Sigma) \to p_{z_0}$. Thus, at the late stages of mixing, it is clear that only the first two moments of ξ characterize the entire, approximately-Gaussian, probability density function of ξ and the beta PDF and mapping closure are consistent (for $\xi' \to 0$).

3.2. *Reactive scalar mixing*

In the flamelet regime, the mapping function of the j-th scalar, Y_j, depends only on a single reference field and can be obtained from the flamelet equations and the mapping function of the passive scalar (Cha 2001). Analogous to the passive scalar case, the mapping functions Y_j allow multi-point information at scales below $\langle(\cdot)\rangle$ to be determined from multi-point information about the reference field, *e.g.*, $\nabla\psi_j = (\partial Y_j/\partial z_0)\nabla z_0$. Whence,

$$\langle \mathcal{D}(\nabla\psi_j)^2 | \psi_j = \phi\rangle = \frac{\langle\chi\rangle}{2}\frac{(\partial Y_j/\partial z_0)^2}{\langle(\partial X/\partial z_0)^2\rangle} \tag{3.4a}$$

$$p_{\psi_j} = \frac{1}{|\partial Y_j/\partial z_0|}p_{z_0} \tag{3.4b}$$

follow, analogous to (3.2). With given Y_j and X, the time-scale ratio of a reactive to a passive scalar can be readily written as

$$T_j/T \equiv \frac{\langle\psi_j'^2\rangle/\langle\chi_j\rangle}{\langle\xi'^2\rangle/\langle\chi\rangle} = \frac{\langle\psi_j'^2\rangle/\langle(\partial Y/\partial z_0)^2\rangle}{\langle\xi'^2\rangle/\langle(\partial X/\partial z_0)^2\rangle} \tag{3.5}$$

or, in terms of the flamelet solution, as (Cha 2001)

$$\frac{T_j}{T} = \frac{\langle\psi_j'^2\rangle}{\langle\xi'^2\rangle}\frac{\langle(\partial X/\partial z_0)^2\rangle}{\int_{-\infty}^{+\infty}(\partial\psi_j/\partial\xi)^2(\partial X/\partial z_0)^2 p_{z_0}dz_0} \ . \tag{3.6}$$

Here, ψ_j is taken to be the steady flamelet solution, which would allow T_j/T to be pretabulated in practice. The mapping function of the passive scalar, X, is given by (3.3*a*.

Implementations of the flamelet equations (steady or unsteady) usually employ additional, simplifying assumptions to model $\chi(t,\xi)$, the local mixing orthogonal to the reaction zone, *i.e.*, in ξ phase space. No entirely satisfactory method of accounting for intermittency effects in a flamelet approach currently exists. The present work is no exception: As is traditionally done, the local, instantaneous scalar dissipation rate is replaced by the spatial average conditional on mixture fraction, thereby neglecting intermittency effects. For all practical purposes, the resulting flamelet model would be constrained by the same limitations as the quasi-steady conditional-moment closure model (Cha & Kosály 2000).

3.3. *Implementation issues*

Implementation issues of (3.6) in Lagrangian particle Monte Carlo calculations, for the joint FDF of the reactive scalars say, are described. The T_j/T ratio can be pretabulated as a function of $\langle\xi\rangle$, ξ', and $\langle\chi\rangle$. During the LES calculation, $\langle\xi\rangle$ and ξ' are known in each computational cell from the subgrid-scale FDF. Well-known models exist for $\langle\chi\rangle$. Then, for a given computational cell, the T_j/T ratio simply multiplies the passive scalar time scale to obtain the time scale to be used for the j-th reacting scalar for a given particle interaction model.

The restriction imposed by the quasi-steady flamelet assumption, namely that the time scale for $\langle\chi\rangle$ be much greater than the time taken for the unsteady flamelet solution to relax to its steady counterpart (Cha & Kosály 2000), requires an *ad hoc* implementation strategy when this assumption is not met at a particular computational grid point. For example, the effects of extinction are important when $\langle\chi|\xi_{\rm st}\rangle \gtrsim \chi_{\rm q}$; reignition events

ensue when the dissipation rate drops back below χ_q (Cha *et al.* 2001). This hysteresis effect would necessitate a binary "switch" for every computational volume to ensure that the proper time scale was being used in the Monte Carlo simulations to describe reignition by distributed combustion, as discussed in the Introduction to this paper. (Note that the conditional scalar dissipation rate is known from (3.2*a*) and (3.3*a*).) The available time-developing information from the Monte Carlo simulations, *e.g.*, the filtered temperature conditional at ξ_{st}, could then be used to switch back to 3.6 when the flamelet regime is reached in a given computational grid point.

4. Results and discussion

Validation of the time-scale model uses the DNS of the turbulent reacting jet, already described in section 2. At a fixed time, t, the spatially-averaged statistics are calculated using the typical LES grid for this flow used to investigate the presumed beta PDF subgrid mixing model in Wall *et al.* (2000). Here, only results from Favre, or density-weighted, averaging is presented. Define an "LES grid point" as a single fixed point centered within a three-dimensional volume defined by the LES grid. (A "DNS grid point" is of course defined by the DNS calculation (Boersma 1999).) At a fixed axial distance, x, from the jet nozzle, a "sliding" filter is used to maximize the use of the DNS data, as is conventionally done for *a priori* validation studies of LES models. That is, each DNS grid point also corresponds to an LES grid point with consecutive LES volumes then overlapping. For the present study, we are interested in a subset of these LES grid points that contain the stoichiometric isosurface. For a given x, define an index I to label a DNS grid point following the stoichiometric isocontour, $\xi = \xi_{st}$, in the azimuthal direction. This will also correspond to an LES grid point due to the sliding filter. Two sets of calculations are performed: one in which the exact local values of ξ^- and ξ^+ from the ensemble of DNS points at an LES grid point are used, and a second set of calculations where ξ^- and ξ^+ are set to zero and one, respectively. The values for ξ^- and ξ^+ will be unique for a given I and will generally vary with I.

Figure 2 shows the volume-averaged scalar dissipation rates of ξ and ψ_P along the stoichiometric isocontour, indexed by I, at various axial distances from a jet nozzle of diameter D. Results are at the same instant of time as figure (1). Symbols are the spatially-averaged DNS data, solid lines are modeling results using the exact local values of ξ^- and ξ^+ within each LES volume, and dash-dash lines are modeling results with $\xi^- = 0$ and $\xi^+ = 1$. The spatially-filtered dissipation rate of ξ would be input into the model in practice. Here, $\langle\chi\rangle$ is calculated directly from the DNS data to circumvent any errors that could be made with the usual LES modeling, *i.e.*, neglecting its transient response to the large-scale mixing. In the near-field of the jet ($x/D \lesssim 15$), the turbulence is not fully developed and $\langle\chi\rangle$ is fairly uniform circumnavigating the stoichiometric isocontour (*i.e.*, as a function of I). Approximate axisymmetry can be observed in this region by inspection of figure 1. In the mid-field ($x/D \approx 25$) and far-field ($x/D \approx 35$) regions of the jet, $\langle\chi\rangle$ can fluctuate by an order-of-magnitude with I. The developed turbulent structures in these regions can cause $\langle\chi\rangle$ along some regions of the stoichiometric isocontour to be comparable in magnitude to values found in the near-field of the jet.

Figure 2 shows that the values of ξ^- and ξ^+ can be set to 0 and 1 in (3.3*a*) without significantly influencing the modeling results for the reactive-scalar dissipation rate $\langle\chi_P\rangle = \langle\chi\rangle\langle(\partial Y_P/\partial z_0)^2\rangle/\langle(\partial X/\partial z_0)^2\rangle$. The $\langle\chi_P\rangle$ predictions are generally in good agreement with the spatially-filtered DNS data. In the near-field of the jet, intermittency effects

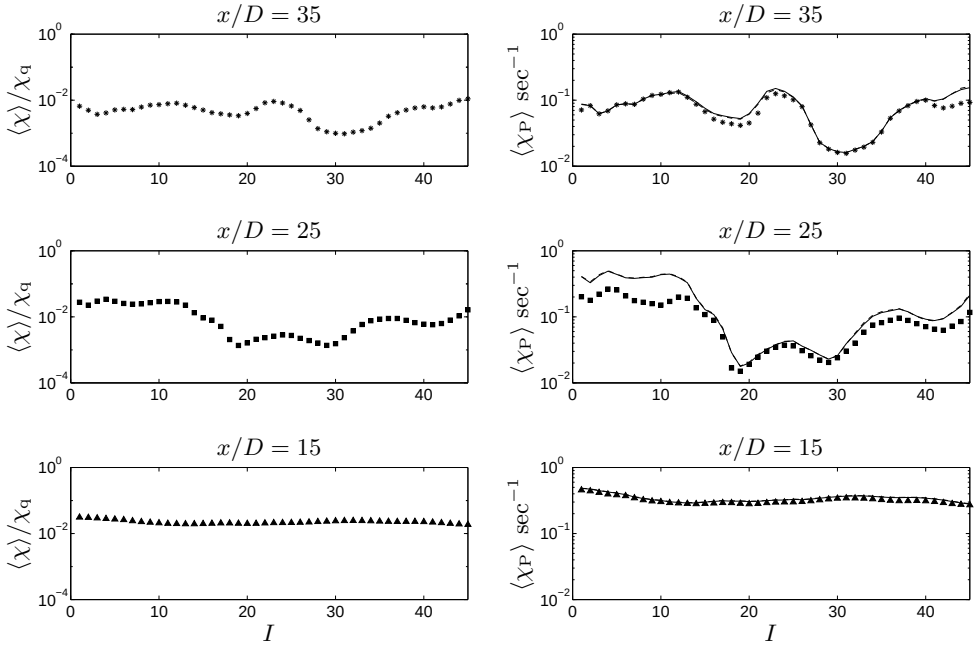

FIGURE 2. Spatially-filtered dissipation rates of the passive scalar, ξ, and the reacting scalar, ψ_P, at three representative axial distances from the jet nozzle: $x/D = 15$ (near-field), $x/D = 25$ (mid-field), and $x/D = 35$ (far-field). Results are at the same instant of time as in figure 1. Symbols are filtered DNS data circumnavigating the stoichiometric isocontour, $\xi = \xi_{st}$, for a given x; I is just a convenient label along the isocontour. Lines are corresponding modeling predictions: Solid lines are modeling results using the exact local values of ξ^- and ξ^+ within each LES volume at a given I, dash-dash lines are modeling results with $\xi^- = 0$ and $\xi^+ = 1$.

are absent and both mapping closure and the present implementation of flamelet modeling are accurate. As is well known, residence-time effects are negligible in the near-field and steady flamelets are valid. Accurate modeling predictions of $\langle\chi_P\rangle$ are thus ensured in the near-field given the validity of the component models (mapping closure and flamelet modeling) used in describing $\langle\chi_P\rangle$.

Some deviations between the $\langle\chi_P\rangle$ data and predictions are seen where the turbulence is developed. Figure 2 shows the representative behavior in the mid-field ($x/D = 25$) and far-field ($x/D = 35$) regions of the jet. In particular, the deviations are conspicuous only for relatively large $\langle\chi\rangle$, and hence for relatively large ξ'.

To investigate the effect of the relatively large $\langle\chi\rangle$ or ξ' on each of the two modeling components (flamelet modeling and mapping closure), the DNS is used to give insight into the subgrid-scale structure of the reacting and passive scalar mixing fields. Figure 3 shows the mass fraction of subgrid-scale product at three representative LES grid points: $x/D = 35$, $I = 45$ (where the maximum deviation between the modeling and filtered data occurs in the far-field region of the jet), at $x/D = 25$, $I = 10$ (where the maximum deviation occurs in figure 2), and at an arbitrary, reference position of $x/D = 25$, $I = 19$ (where good agreement between the modeling and data is seen in figure 2). Also shown are the corresponding local values of $\chi(\xi)$ at the subgrid-scales properly nondimensionalized by χ_q for the present discussion.

With regard to the flamelet model, the neglect of the subgrid-scale spatial fluctuations of χ contributes to the deviations between the filtered DNS data and the modeling predic-

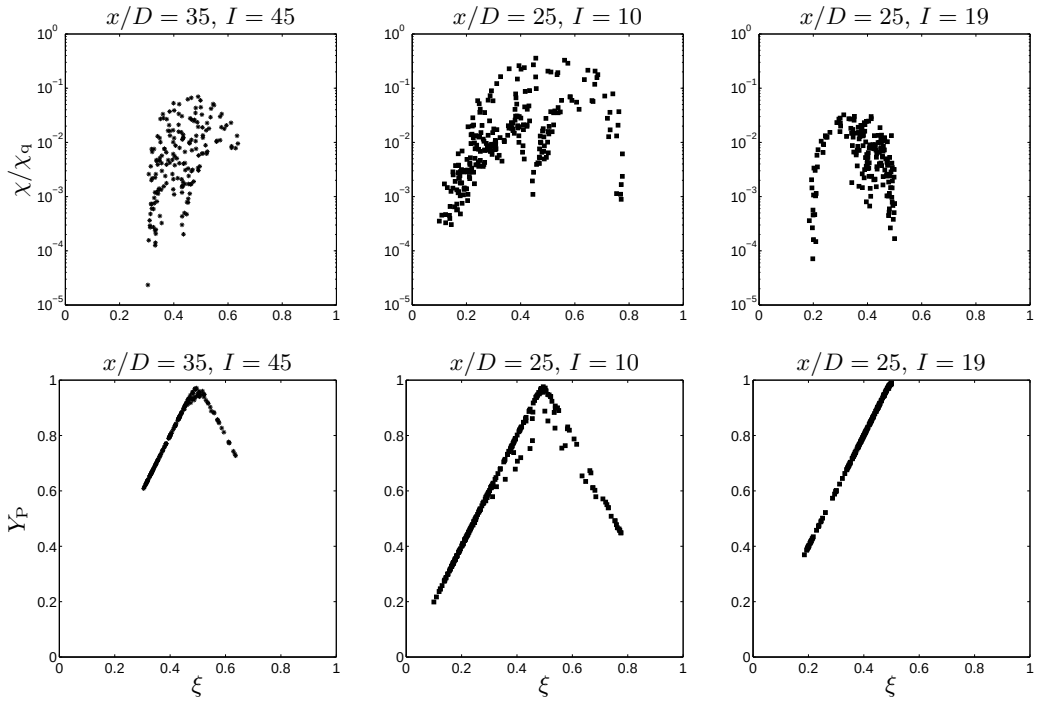

FIGURE 3. Exact subgrid-scale values of χ, the dissipation rate of ξ, and the corresponding local product mass fractions, ψ_P, at three representative LES grid points in figure 2: $x/D = 35$, $I = 45$ (stars), $x/D = 25$, $I = 10$ (squares), and $x/D = 25$, $I = 19$ (squares). The dissipation rate of ξ is nondimensionalized by χ_q, the quenching value of χ for the present chemistry case as defined by the steady flamelet solution.

tions of figure 2. Figure 3 shows that when local values of χ are large, local extinction is observed in the corresponding product mass fractions. Note that locally, $\chi \sim \chi_q$ although $\langle\chi\rangle << \chi_q$ (for subplot $x/D = 25$, $I = 10$), which follows from the fine-scale structure of the dissipation rate. For smaller $\langle\chi\rangle$ (subplots $x/D = 35$, $I = 45$ and $x/D = 25$, $I = 19$), the subgrid-scale fluctuations of χ are not large enough to reach local extinction and the flamelet solution is accurate.

With regard to mapping closure, in regions of the flow where the turbulence is developed and where relatively large values of ξ' occur (subplot $x/D = 25$, $I = 10$ in figure 3), multi-scale mixing processes are occurring. In these regions, a unique set of ξ^+ and ξ^- values misrepresents the true subgrid-scale structure of the mixing. This is because, for developed turbulence, the large difference between global ξ^+ and ξ^-, proportional to ξ', necessarily result in additional length scales corresponding to the distribution of local ξ^- and ξ^+. Thus, ξ^- and ξ^+ as defined by mapping closure less accurately represents the true subgrid-scale mixing.

With RANS turbulence modeling, the effect of neglecting the true values of ξ^- and ξ^+ had a negligible influence on the modeling results (Cha & Trouillet 2002): At a given $\boldsymbol{x}$, for time-averaged ξ values close to either 0 or 1, the variance of ξ will be small and hence $\xi^+(\boldsymbol{x})$ and $\xi^-(\boldsymbol{x})$ could be set to 1 and 0, respectively. At intermediate $\langle\xi\rangle$ values, the effect of intermittency drives $\xi^- \to 0$ and $\xi^+ \to 1$ in the statistically stationary limit, and again ξ^- and ξ^+ could be set to 0 and 1 without significantly influencing modeling results within a RANS turbulence modeling framework. Here, for the LES case, accounting for

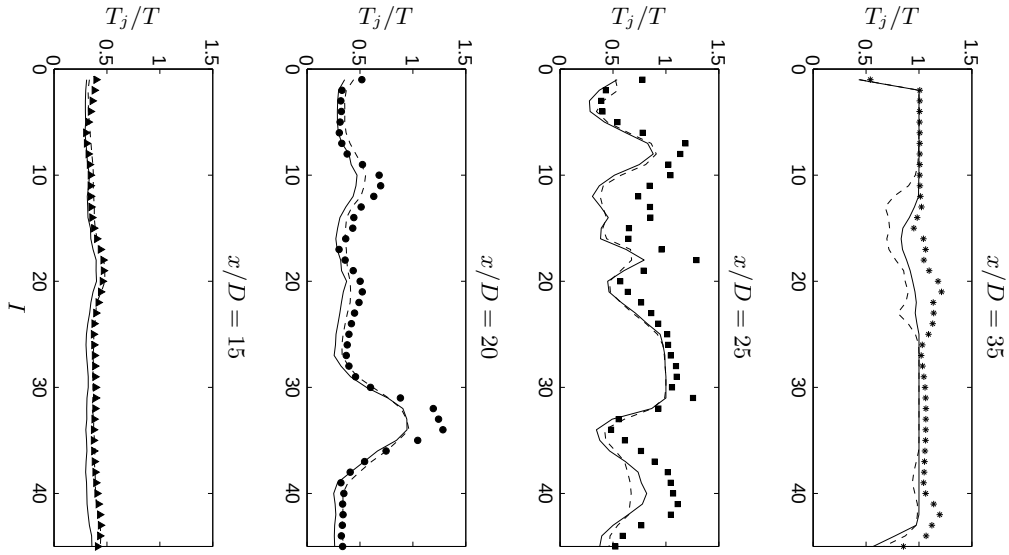

FIGURE 4. Time scale ratio of the reactive to passive scalar for increasing axial distances from the jet nozzle, from $x/D = 15$ to $x/D = 35$, the approximate time-averaged stoichiometric flame-length. Symbols are filtered DNS data. Lines are corresponding modeling predictions: Solid lines are modeling results using the exact local values of ξ^- and ξ^+ within each LES volume at a given I, dash-dash lines are modeling results with $\xi^- = 0$ and $\xi^+ = 1$.

(spatial) intermittency effects can sometimes be important when the subgrid variance of ξ is sufficiently large, as illustrated above. For the typical LES grid spacing employed in the present case (Wall *et al.* 2000), the subgrid variance is generally small and the effect of neglecting ξ^- and ξ^+ has negligible impact on the overall modeling performance. In practice, the expectation is that ξ^- and ξ^+ can be set to 0 and 1 in (3.3) as the subgrid-scale variance of ξ will generally be small in a large-eddy simulation.

Figure 4 shows the modeling predictions (lines) of the time scale ratio, (3.6), versus the experimental data obtained from the filtered DNS (symbols). The comparisons are made for the same grid points as in figure 2 (and for the same axial distances as in the RANS case of Cha & Trouillet (2002)). Again, solid lines are modeling results using the exact local values of ξ^- and ξ^+ within each LES volume at a given I, and dash-dash lines are modeling results with $\xi^- = 0$ and $\xi^+ = 1$. As was also seen in the reactive scalar dissipation rate predictions, ξ^- and ξ^+ can be set to 0 and 1 in (3.3a) without significantly influencing the modeling results, here for the time scale ratio. The T_j/T predictions are in excellent agreement in the near-field of the jet. The deviations in the mid- and far-fields of the jet occur when ξ' or $\langle\chi\rangle$ is sufficiently large, which follows directly from the above discussion of Figs. 2 and 3. Overall, the results show that T_j can be significantly less than T, even in the mid- and far-field regions of the jet for the LES case. The new modeling represents a significant improvement over simply approximating T_j by T alone.

5. Summary and conclusions

Transported probability-density-function approaches for the large-eddy PDF, known as the "filtered density function approach" (FDF), require modeling of the mixing processes at the subgrid-scale. For large-eddy simulations of initially nonpremixed turbulent

reacting flows, the current FDF approaches can, strictly, treat only distributed combustion (small Damköhler number flows) because of the limitations imposed by neglecting the effects of chemistry on the mixing process. Thus many problems of practical engineering interest, where Arrhenius kinetics are used and the chemistry is relatively fast, are beyond the reach of FDF. The merits of the FDF approach include the potential to describe local reignition events among others. To describe local extinction from a mixing-limited combustion mode, the model must first be able to treat flamelet combustion, by definition. A model for the time scale of reactive scalar mixing at the subgrid-scale that is valid both for flamelet and distributed combustion has been developed, (3.6) in this paper. The model is based on mapping closure, to describe the subgrid-scale mixing of the passive scalar, and flamelet modeling, to describe the mixing of the reactive scalars in mixture fraction space. Application to Lagrangian particle Monte Carlo calculations has been described.

The modeling results using spatially-filtered DNS data of a turbulent reacting jet (with one-step, Arrhenius chemical kinetics, and heat release) show generally good predictions of the reactive scalar time scale, which can be significantly less than the passive scalar time scale even in the mid-field regions of the jet. Mapping closure does not account for intermittency, nor does the present, conventional implementation of steady flamelet modeling needed to obtain the reactive scalar mapping functions. In regions of the jet flame where the turbulence is developed and the subgrid variance and dissipation rate of the passive scalar are relatively large, some deviation between the data and modeling predictions occur.

Acknowledgements

The authors express gratitude to Bendiks Boersma for making his DNS database available to us.

REFERENCES

Bilger, R. W. 1980 Turbulent flows with nonpremixed reactants. In *Turbulent Reacting Flows*, *Topics in Applied Physics* 44, chap. 3, pp. 65–113. Springer.

Boersma, B. J. 1999 Direct numerical simulation of a turbulent reacting jet. *Annual Research Briefs*, Center for Turbulence Research, NASA Ames/Stanford Univ., pp. 59–72.

Cha, C. M. 2001 Transported pdf modeling of turbulent nonpremixed combustion. *Annual Research Briefs*, Center for Turbulence Research, NASA Ames/Stanford Univ., pp. 79–86.

Cha, C. M. & Kosály, G. 2000 Quasi-steady modeling of turbulent nonpremixed combustion. *Combust. Flame* **122**, 400–421.

Cha, C. M., Kosály, G. & Pitsch, H. 2001 Modeling extinction and reignition in turbulent nonpremixed combustion using a doubly-conditional moment closure approach. *Phys. Fluids* **13**, 3824–3834.

Cha, C. M. & Trouillet, P. 2002 A model for the mixing time scale of a turbulent reacting scalar. *Phys. Fluids* (submitted).

Chen, H., Chen, S. & Kraichnan, R. H. 1989 Probability distribution of a stochastically advected scalar field. *Phys. Rev. Lett.* **63**, 2657–2660.

Colucci, P. J., Jaberi, F. A., Givi, P. & Pope, S. B. 1999 Filtered density function for large eddy simulation of turbulent reacting flows. *Phys. Fluids* **10**, 499–515.

Cook, A. W. & Riley, J. J. 1994 A subgrid model for equilibrium chemistry in turbulent flows. *Phys. Fluids* **6**, 2868–2870.

Cook, A. W. & Riley, J. J. 1997 Subgrid-scale modeling for turbulent, reacting flows. *Combust. Flame* **112**, 593–606.

Cook, A. W., Riley, J. J. & Kosály, G. 1997 A laminar flamelet approach to subgrid-scale chemistry in turbulent flows. *Combust. Flame* **109**, 332–341.

Domingo, P. & Vervisch, L. 1996 Triple flames and partially premixed combustion in autoignition of non-premixed turbulent mixtures. *Proc. Combust. Inst.* **26**, 233–240.

Dopazo, C. 1975 Probability density function approach for a turbulent axisymmetric heated jet. Centerline evolution. *Phys. Fluids A* **18**, 397–404.

Gao, F. 1991*a* An analytical solution for the scalar probability density function in homogeneous turbulence. *Phys. Fluids A* **3**, 511–513.

Gao, F. 1991*b* Mapping closure and non-Guassianity of the scalar probability density functions in isotropic turbulence. *Phys. Fluids A* **3**, 2438–2444.

Gao, F. & O'Brien, E. E. 1993 A large-eddy simulation scheme for turbulent reacting flows. *Phys. Fluids* **5**, 1282–1284.

Girimaji, S. S. 1991 Assumed β-pdf model for turbulent mixing: Validation and extension to multiple scalar mixing. *Combust. Sci. and Tech.* **78**, 177–196.

Hewson, J. C. & Kerstein, A. R. 2001 Stochastic simulation of transport and chemical kinetics in turbulent $CO/H_2/N_2$ flames. *Combust. Theory Modelling* **5**, 669–697.

Jaberi, F. A., Colucci, P. J., James, S., Givi, P. & Pope, S. B. 1999 Filtered mass density function for large-eddy simulation of turbulent reacting flows. *J. Fluid Mech.* **401**, 85–121.

Norris, A. T. & Pope, S. B. 1991 Turbulent mixing model based on ordered pairing. *Combust. Flame* **83**, 27–42.

O'Brien, E. E. & Jiang, T. L. 1991 The conditional dissipation rate of an initially binary scalar in homogeneous turbulence. *Phys. Fluids A* **3**, 3121–3123.

Peters, N. 1984 Laminar diffusion flamelet models in non-premixed turbulent combustion. *Prog. Energy Combust. Sci.* **10** (3), 319–339.

Pitsch, H., Cha, C. M. & Fedotov, S. 2002 Flamelet modeling of non-premixed turbulent combustion with local extinction and re-ignition. *Combust. Theory Modelling* (submitted).

Pitsch, H. & Steiner, H. 2000*a* Large-eddy simulation of a turbulent piloted methane/air diffusion flame (Sandia flame D). *Phys. Fluids* **12**, 2541–2554.

Pitsch, H. & Steiner, H. 2000*b* Scalar mixing and dissipation rate in large-eddy simulations of non-premixed turbulent combustion. *Proc. Combust. Inst.* **28**, 41–49.

Pope, S. B. 1985 PDF methods for turbulent reacting flows. *Prog. Energy Combust. Sci.* **11**, 119–192.

Pope, S. B. 1990 Computations of turbulent combustion: Progress and challenges. *Proc. Combust. Inst.* **23**, 591–612.

Pope, S. B. 2000 *Turbulent Flows*. Cambridge.

Sabel'nikov, V. A. & Gorokhovski, M. 2001 Extended LMSE and Langevin models of the scalar mixing in the turbulent flow. In *Second International Symposium on Turbulence and Shear Flow Phenomena*. Royal Institute of Technology (KTH), Stockholm, Sweden, vol. 3, pp. 257–262.

Sripakagorn, P., Kosály, G. & Pitsch, H. 2000 Local extinction-reignition in turbulent nonpremixed combustion. *Annual Research Briefs*, Center for Turbulence Research, NASA Ames/Stanford Univ., pp. 117–128.

Wall, C., Boersma, B. J. & Moin, P. 2000 An evaluation of the assumed beta probability density function subgrid-scale model for large eddy simulation of nonpremixed turbulent combustion with heat release. *Phys. Fluids* **12**, 2522–2529.